HP-Multigrid as Smoother algorithm for higher order discontinuous Galerkin discretizations of advection dominated flows

Jaap van der Vegt

Mathematics of Computational Science Group
Department of Applied Mathematics
University of Twente

Enschede, The Netherlands

Joint work with Sander Rhebergen

Part 4.

USTC Summer School, August 29 – September 2, 2022

Introduction

Motivation:

- Develop efficient multigrid algorithms for space-(time) discontinuous Galerkin finite element discretizations of advection dominated flows.

Main Features of Space-Time DG Methods

- Simultaneous discretization in space and time: time is considered as an additional dimension to the spatial dimensions.
- Discontinuous basis functions, both in space and time, are used with only a weak coupling across element faces resulting in an extremely local, element based discretization.
- The space-time DG method is closely related to the Arbitrary Lagrangian Eulerian (ALE) method.

Benefits of Space-Time DG Methods

- A locally conservative discretization is obtained on moving and deforming meshes for conservative pde's.
- Well suited for *hp*-adaptation and parallel computations.
- Space-time formulations are well suited for problems which require dynamic meshes, such as free surface problems, multifluid flows, and fluid-structure interaction.
- No data interpolation or extrapolation is necessary at free boundaries and after mesh movement or adaptation.

Disadvantages of Space-Time DG Methods

- The space-time DG method generally results in an implicit formulation, which requires the solution of a system of algebraic equations.

Applications

- Compressible and incompressible Euler and Navier-Stokes equations, e.g. fluid-structure interaction and free surface problems
- Multifluid flows using two-fluid elements
- Dispersed multiphase flows
- Free surface gravity waves

Computational Efficiency

- The computational cost of solving the (non)linear algebraic system resulting from a DG discretization with a multigrid or other iterative method is considerable and needs to be reduced.

- In particular, for higher order accurate DG discretizations of advection dominated flows with thin boundary layers convergence rates are unsatisfactory.

Objectives

- To investigate multigrid performance for higher order space-time discontinuous Galerkin discretizations of advection dominated flows using a detailed multilevel analysis.
- To improve multigrid performance by optimizing the multigrid smoother by minimizing the operator norm and spectral radius of the multigrid error transformation operator.
- To investigate the theoretically obtained results on realistic test cases.

Outline of Presentation

- Multilevel analysis and optimization of multigrid performance
- Performance of optimized multigrid algorithms
- Conclusions

Solution Strategies for Implicit DG Discretizations

Main solution techniques for solving implicit DG discretizations

- Newton multigrid methods with ILU smoother in combination with GMRES
- FAS multigrid in combination with explicit pseudo-time integration methods

For industrial applications, both approaches need significant improvements for higher order DG discretizations, both in terms of computing time and memory use.

Pseudo-time Integration

- Let the system of algebraic equations of the space-time DG discretization at time level n be denoted as
$$N_h \widehat{U}_h^n = F_h.$$
- A pseudo time derivative is added to the system, which is integrated to steady-state in pseudo-time
$$\frac{\partial \widehat{U}_h^*}{\partial \tau} = -\frac{1}{\triangle t}(N_h \widehat{U}_h^* - F_h).$$
- At steady state $\widehat{U}_h^n = \widehat{U}_h^*$.
- Convergence to steady state in pseudo-time is accelerated using a multigrid algorithm with a Runge-Kutta type smoother.
- Since time-accuracy is not important in pseudo-time there is a lot of room to optimize the Runge-Kutta smoother in the multigrid algorithm.

- For explicit or point-implicit RK smoothers the pseudo-time approach is easy to implement, has minimal memory overhead and, due to its locality, combines well with discontinuous Galerkin discretizations.

- Explicit and point-implicit smoother are very easy to use for non-linear problems in combination with a FAS multigrid algorithm.

- The algorithm works reasonably well for second order accurate DG discretizations of the (in)compressible Euler and Navier-Stokes equations, but not for higher order accurate DG discretizations.

The aim is to find new multigrid algorithms, which also work well for higher order accurate discretizations of advection dominated flows, including thin boundary layers.

Multigrid Performance

Multigrid performance is affected by:

- Efficiency of iterative solver in reducing high-frequency error components
- Coarse grid discretization
- Transfer of data between coarse and fine meshes

Approach

- Perform extensive multi-level Fourier analysis of multigrid algorithms for space-time DG discretizations using various smoothers, e.g. ILU, SSOR, Runge-Kutta methods.
- Investigate different coarse grid discretizations.
- Improve multigrid performance by optimizing free coefficients in the smoother and other multigrid parameters.
- All discrete Fourier analysis results are verified using matrix analysis.

  The matrix analysis also allows the investigation of the effect of boundary conditions, but is too expensive to be used in multigrid optimization.

Advection-Diffusion Equation

Model problem:

- The space-time discretization for the advection-diffusion equation

$$\frac{\partial u}{\partial t} + a \cdot \nabla u = \nu \Delta u$$

  can be represented by the linear system

$$L_h \widehat{U}_h^n = F_h.$$

- The discretization depends on the flow angle and the dimensionless numbers

$$CFL = \frac{|a| \triangle t}{h}, \quad Re_h = \frac{|a| h}{\nu}$$

Standard *hp*-Multigrid

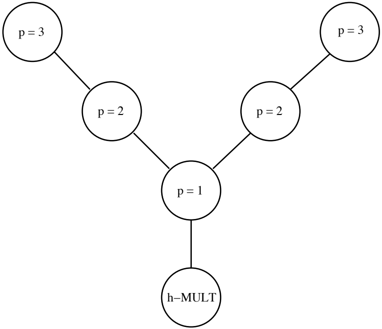

- Combination of p-multigrid with h-multigrid at the lowest polynomial level ($p = 1$).
- Note, use $p = 0$ in coarsest mesh is not advisable.

Multigrid Convergence rates

- For linear problems the multigrid error is controlled by the multigrid error transformation operator
$$e_h^1 = M_{nh,p} e_h^0.$$

- An upper bound for the error and residual after one full multigrid cycle is
$$\|e_h^1\| \leq \|M_{nh,p}\| \|e_h^0\|,$$
$$\|d_h^1\| \leq \|L_h M_{nh,p} L_h^{-1}\| \|d_h^0\|,$$
where the operator norm is defined as
$$\|M_{nh,p}\| := \sup_{e_h^0 \neq 0} \frac{\|M_{nh,p} e_h^0\|}{\|e_h^0\|},$$
with an analogous definition for $\|L_h M_{nh,p} L_h^{-1}\|$.

- The asymptotic convergence rate of the multigrid algorithm is given by the spectral radius of $M_{nh,p}$.

Multigrid Optimization with Runge-Kutta Smoothers

- The multigrid performance is optimized by searching for Runge-Kutta smoother coefficients such the operator norm $\|M_{nh,p}\|$ or the spectral radius of $\rho(M_{nh,p})$ is minimized.
- The optimization is performed under the constraint that the spectral radius of the multigrid error transformation operator and the smoother for all p-levels is less than one.
- In order to compute the operator norms and spectral radii efficiently discrete Fourier analysis is used.

Discrete Fourier Analysis in 2D

- Consider the infinite mesh G_h, defined in $\mathbb{R}^2$ as

$$G_h := \left\{(x_1, x_2) = (k_1 h_1, k_2 h_2) \mid k \in \mathbb{Z}^2, h \in \left(\mathbb{R}^+\right)^2\right\}.$$

- Define the Fourier space

$$\mathcal{F}(G_h) := \operatorname{span}\left\{e^{i\theta\cdot x/h} \mid \theta \in \Theta := [-\pi, \pi)^2, x \in G_h\right\}$$

  contains any bounded infinite grid function.

- Due to aliasing, Fourier components with $|\hat{\theta}| := \max\{|\theta_1|, |\theta_2|\} \geq \pi$ are not visible on G_h.

- For each $v_h \in \mathcal{F}(G_h)$ there exists a Fourier transformation, hence $v_h(x)$ can be written as a linear combination of Fourier components

$$v_h(x) = \int_{|\theta| \leq \pi} \widehat{v}_h(\theta) e^{i\theta \cdot x/h} d\theta, \qquad x \in G_h,$$

with inverse transformation

$$\widehat{v}_h(\theta) = \frac{1}{4\pi^2} \sum_{x \in G_h} v_h(x) e^{-i\theta \cdot x/h}, \qquad -\pi \leq \theta_j < \pi,$$

Three-level Discrete Fourier Analysis

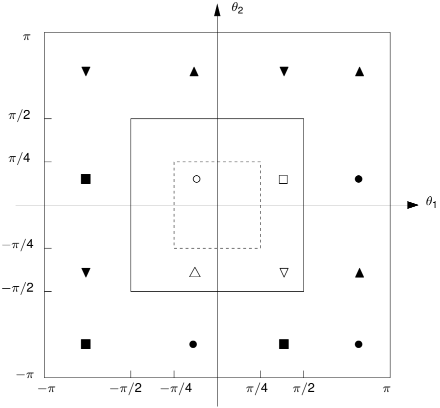

Aliasing modes for three-level discrete Fourier analysis on uniformly coarsened mesh.

Main Steps Discrete Fourier Multilevel Analysis

The main steps in the discrete Fourier analysis can be summarized as:

- Compute for each mesh and polynomial level the discrete Fourier symbol of the DG discretization and smoother. (Three p- and three h-levels are used in the Fourier analysis).
- Compute the discrete Fourier symbol of the mesh transfer operators, viz. restriction and prolongation operators. These operators result in a coupling of modes.
- Combine all individual operators into the multigrid error transformation operator. This results in the Fourier symbol of the *hp*-error transformation operator $\widehat{M}_{nh,p}$.
- For a 2D steady state problem with a fourth order accurate space-time DG discretization of the advection-diffusion equation this requires for each Fourier mode the solution of an eigenvalue problem with a 160×160 matrix.

- Compute for each Fourier mode the spectral radius of the error transformation operator.

- The operator norm $\|M_{nh,p}\|$ can be linked to its discrete Fourier transform

$$\|M_{nh,p}\| = \sup_{\theta \in \Theta_{nh,p} \setminus \Psi_{nh,p}} \sqrt{\rho\big(\widehat{M}_{nh,p}(\theta)\big(\widehat{M}_{nh,p}(\theta)\big)^{*}\big)}$$

- The asymptotic convergence factor is given by the spectral radius

$$\mu_e = \sup_{\theta \in \Theta_{nh,p} \setminus \Psi_{nh,p}} \rho\big(\widehat{M}_{nh,p}(\theta)\big)$$

Point-Implicit Runge-Kutta Method

Since point-implicit Runge-Kutta methods combine very well with FAS multigrid we first explore these algorithms.

- The point-implicit Runge-Kutta method is defined as

$$w_0 = w^l_{nh,p}$$

$$(I + \lambda_\sigma \beta_{ii}) w_i = w_0 - \sum_{j=0}^{i-1} \big(\beta_{ij} w_j + \alpha_{ij} \lambda_\sigma (L_{nh,p} w_j - f_{nh,p})\big), \quad i = 1, \cdots, 5,$$

$$w^{l+1}_{nh,p} = w_5,$$

  with α_{ij} Runge-Kutta coefficients, $\lambda_\sigma = \triangle\sigma / \triangle\tau$, and $\triangle\sigma$ the pseudo-time step.

- At the steady state of the σ-pseudo-time integration we obtain the solution of $L_{nh,p} u_{nh,p} = f_{nh,p}$.

- The point-implicit Runge-Kutta method is straightforward to use for nonlinear problems.

Optimization of Runge-Kutta Smoothers

- The only requirement we impose on the Runge-Kutta coefficients α_{ij} and β_{ij} is that the algorithm is first order accurate in pseudo-time.

- In particular, this implies the consistency condition

$$\sum_{j=0}^{4} \alpha_{5j} = 1.$$

- All other Runge-Kutta coefficients can be optimized to improve the pseudo-time convergence in combination with the multigrid algorithm.

- The RK smoother coefficients are optimized separately for each *p*-level.

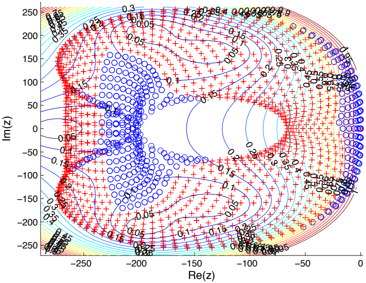

$p = 1$

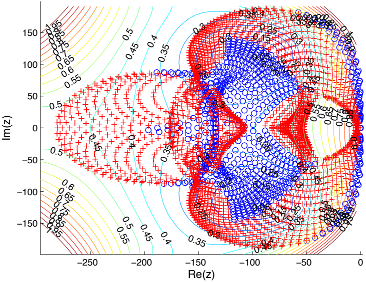

$p = 2$

Stability domain of point-implicit smoothers for three-level *hp*-multigrid at steady state ($Re_h = 10.000$)

Three-level *hp*-Multigrid

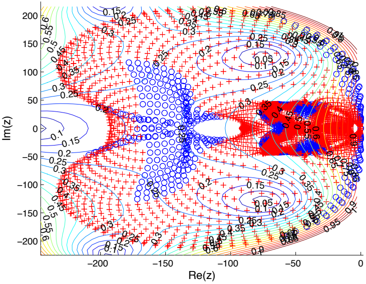

Smoother $p = 3$

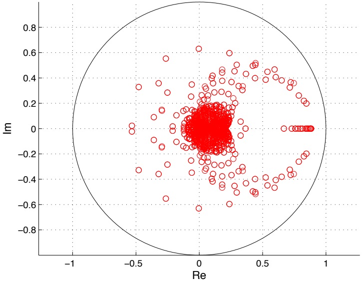

TLA

Stability domain of point-implicit smoothers for three-level *hp*-multigrid at steady state ($Re_h = 10.000$, $\rho(TLA) = 0.88326$, $\|M_{TLA}\| = 0.89250$, $\rho_{GMRES} = 0.73822$).

Stretched Meshes

- The *hp*-multigrid convergence rapidly deteriorates on stretched meshes which are necessary to capture boundary layers.

- Also, for uniform meshes the performance of *hp*-multigrid has room for improvement

ILU-Smoother

Remark:

- Multigrid convergence is much better for higher order DG discretizations with an ILU smoother.
- The ILU smoother requires, however, a large fill-in of 7 to 10 times the original matrix for the considered problems, and is not really practical for large scale problems

hp-Multigrid as Smoother Algorithm

The *hp*-multigrid performance for higher order DG discretizations is improved using the following steps:

- *h*-Multigrid, combining uniform and semi-coarsened meshes, is used as smoother in the *p*-multigrid at all *p*-levels, resulting in the *hp*-Multigrid as Smoother algorithm.
- A low cost semi-implicit Runge-Kutta smoother is introduced to deal with boundary layers and highly stretched meshes.

hp-MGS Multigrid

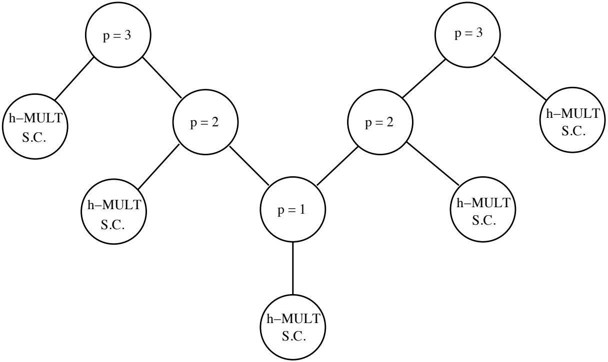

- *hp*-multigrid with semi-coarsening Multigrid as Smoother algorithm at all *p*-levels

MGS-Algorithm

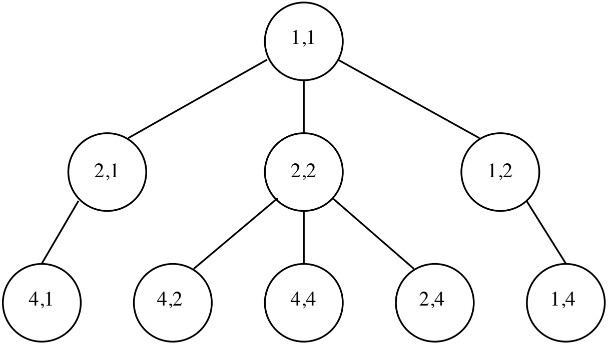

- Multigrid as Smoother algorithm with semi-coarsening in x- and y-direction

Semi-Implicit Runge-Kutta Method

- The semi-coarsening multigrid and the block matrix structure of the DG discretization combine well with a semi-implicit Runge-Kutta method.

- Split the matrix $L_{nh,p}$, when sweeping in the local i_1-direction, as

$$L_{nh,p} = L_{nh,p}^{i_{11}} + L_{nh,p}^{i_{12}},$$

  and for sweeps in the local i_2-direction as

$$L_{nh,p} = L_{nh,p}^{i_{21}} + L_{nh,p}^{i_{22}}.$$

Semi-Implicit Runge-Kutta Method

- The semi-implicit Runge-Kutta method for sweeps in the local i_1-direction can be defined as

$$
\begin{aligned}
w_0 &= w^l_{nh,p} \\
w_k &= \left(I_{nh,p} + \beta_k \lambda_\sigma L^{i_{11}}_{nh,p}\right)^{-1}\left(w_0 - \sum_{j=0}^{k-1} \alpha_{kj}\lambda_\sigma\left(L^{i_{12}}_{nh,p} w_j - f_{nh,p}\right), \quad k = 1, \cdots, 5, \\
w^{l+1}_{nh,p} &= w_5,
\end{aligned}
$$

- The semi-implict Runge-Kutta method results in a set of uncoupled block-tridiagonal linear systems on a structured mesh.

- At steady state of the σ-pseudo-time integration we obtain the solution of $L_{nh,p} u_{nh,p} = f_{nh,p}$.

- For $p = 3$ and steady state problems we need to optimize 45 Runge-Kutta coefficients.

hp-MGS Error Transformation Operator

- The initial error and the error after one application of the multigrid algorithm are related as
$$e^1_{nh,p} = M_{nh,p} e^0_{nh,p},$$
with $M_{nh,p}$ the *hp-MGS* multigrid error transformation operator.

- The *hp-MGS* multigrid error transformation operator $M_{nh,p}$ can be defined recursively as

$$\begin{aligned} M_{nh,p} &= \left(HU_{nh,p}\right)^{\nu_2}\left(I_{nh,p} - T^{p}_{nh,p-1}(I_{nh,p-1} - M_{nh,p-1})(L_{nh,p-1})^{-1}\right. \\ &\qquad \left. Q^{p-1}_{nh,p} L_{nh,p}\right)\left(HU_{nh,p}\right)^{\nu_1} && \text{if } p > 1, \\ &= HU_{nh,1} && \text{if } p = 1. \end{aligned}$$

h-MGS Error Transformation Operator

- The *h-MGS* error transformation operator $HU_{nh,p}$ is equal to

$$
\begin{aligned}
HU_{nh,p} &= (HS^1_{nh,p} HS^2_{nh,p})^{\gamma} (I_{nh,p} - P^{nh}_{2nh,p}(I_{2nh,p} - HU_{2nh,p}) \\
&\quad (L_{2nh,p})^{-1} R^{2nh}_{nh,p} L_{nh,p})(HS^2_{nh,p} HS^1_{nh,p})^{\gamma}, && \text{if } n < m, \\
&= 0, && \text{if } n = m.
\end{aligned}
$$

Semi-Coarsening Smoother Error Transformation Operator

- The semi-coarsening multigrid error transformation operators $HS^1_{nh,p}$ and $HS^2_{nh,p}$, are equal to

$$
\begin{aligned}
HS^1_{nh,p} = & (S^1_{nh,p})^{\mu_2}\,(I_{nh,p} - P^{nh}_{(2n_1,n_2)h,p}(I_{(2n_1,n_2)h,p} - HS^1_{(2n_1,n_2)h,p}) \\
& \quad (L_{(2n_1,n_2)h,p})^{-1} R^{(2n_1,n_2)h}_{nh,p} L_{nh,p})\,(S^1_{nh,p})^{\mu_1}, && \text{if } n < m, \\
= & \, 0, && \text{if } n = m, \\
HS^2_{nh,p} = & (S^2_{nh,p})^{\mu_2}\,(I_{nh,p} - P^{nh}_{(n_1,2n_2)h,p}(I_{(n_1,2n_2)h,p} - HS^2_{(n_1,2n_2)h,p}) \\
& \quad (L_{(n_1,2n_2)h,p})^{-1} R^{(n_1,2n_2)h}_{nh,p} L_{nh,p})\,(S^2_{nh,p})^{\mu_1}, && \text{if } n < m, \\
= & \, 0, && \text{if } n = m.
\end{aligned}
$$

- The error transformation operator is analyzed using discrete Fourier analysis (three p-levels and three uniformly and semi-coarsened h-levels) for the 2D advection-diffusion equation.

Discrete Fourier Multilevel Analysis of *hp-MGS* Algorithm in 2D

The following complications arise in the discrete Fourier analysis of the *hp-MGS* algorithm

- The Fourier modes on the uniformly and semi-coarsened meshes have different aliasing properties.
- Fourier symbols on the uniformly and semi-coarsened meshes must be combined, which is complicated due to aliasing.
- Large number of multigrid levels, three *p*-levels and three uniformly and semi-coarsened mesh levels.

Discrete Fourier Analysis of *hp-MGS Algorithm*

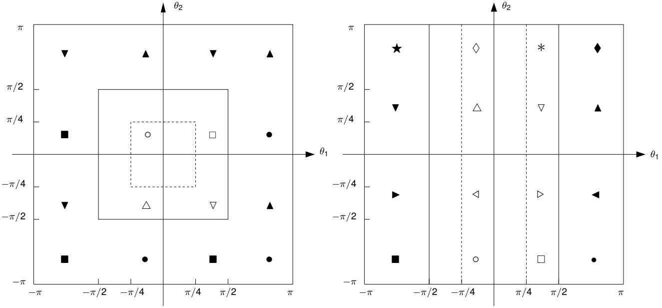

Aliasing modes for three-level discrete Fourier analysis. Left uniform coarsening, right semi-coarsening in x-direction.

Overview Computational Complexity of *hp-MGS* Algorithm

LU^1_{cost}	LU^2_{cost}	LU^3_{cost}	LU^1_{cost}/LU^2_{cost}	LU^1_{cost}/LU^3_{cost}
12326 *NM*	5942 *NM*	5840 *NM*	2.1	2.1

B^1_{cost}	B^2_{cost}	B^3_{cost}	B^1_{cost}/B^2_{cost}	B^1_{cost}/B^3_{cost}
14331 *NM*	2091 *NM*	1773 *NM*	6.9	8.1

Overview of computational complexity of *hp-MGS* algorithm consisting of LU-decomposition cost and cost of forward and backward solution.

Mem^1	Mem^2	Mem^3	Mem^1/Mem^2	Mem^1/Mem^3
3081 *NM*	1551 *NM*	1478 *NM*	2.0	2.1

Overview of memory storage for LU-decomposition matrices in *hp-MGS* algorithm.

(^{1}-*hp-MGS*, ^{2}-only smoother at $p = 2, 3$ levels, ^{3}-*hp*-multigrid).

Multilevel Analysis *hp-MGS* Algorithm, Uniform Meshes

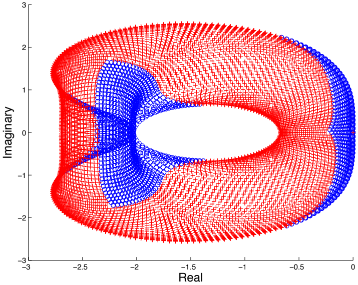

Eigenvalues $L_{h,1}$

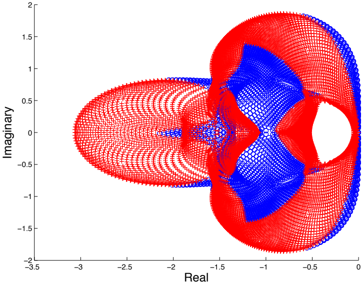

Eigenvalues $L_{h,2}$

Spectra of DG matrices for $p = 1$ and 2.

($Re_{h_1} = Re_{h_2} = 10^3$, $A_h = 1$, $\alpha = 45^\circ$, steady state)

Multilevel Analysis *hp-MGS* Algorithm, Uniform Meshes

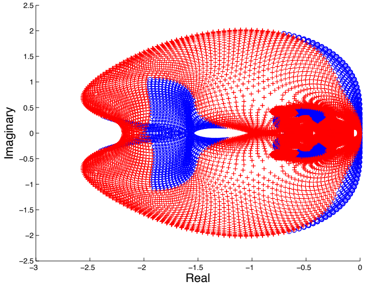

Eigenvalues $L_{h,3}$

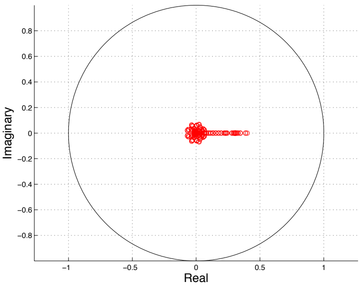

TLA-*hpMGS*

Spectrum of DG matrix $L_{h,3}$ and error transformation operator of *hp-MGS* algorithm.

$(Re_{h_1} = Re_{h_2} = 10^3, A_h = 1, \alpha = 45^\circ$, steady state)

Multilevel Analysis *hp*-Algorithm, Uniform Meshes

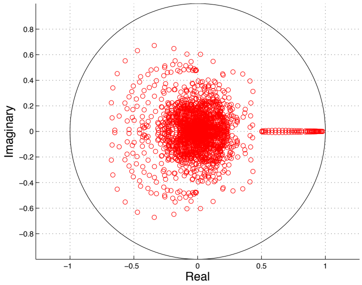

TLA-*hpMGS(1)*

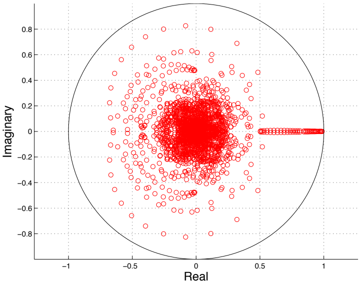

TLA-*hp*

Spectra of error transformation operator of the *hp-MGS(1)* and *hp*-multigrid algorithms.
($Re_{h_1} = Re_{h_2} = 10^3$, $A_h = 1$, $\alpha = 45^\circ$, steady state)

Multilevel Analysis *hp-MGS* Algorithm, Stretched Meshes

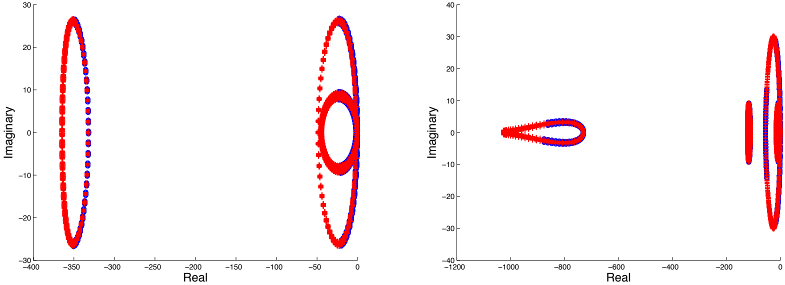

Eigenvalues $L_{h,1}$ Eigenvalues $L_{h,2}$

Spectra of DG matrices for $p = 1$ and 2.

($Re_{h_1} = 10^{-1}$, $Re_{h_2} = 10^3$, $A_h = 100$, $\alpha = 75^\circ$, steady state)

Multilevel Analysis *hp-MGS* Algorithm, Stretched Meshes

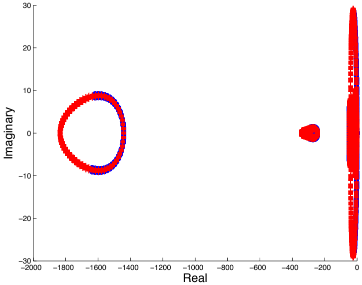

Eigenvalues $L_{h,3}$

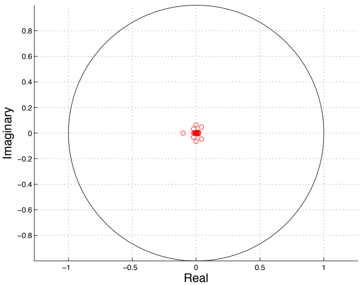

TLA-*hpMGS*

Spectra of DG matrix $L_{h,3}$ and error transformation operator of *hp-MGS* algorithm.

$(Re_{h_1} = 10^{-1}, Re_{h_2} = 10^3, A_h = 100, \alpha = 75^\circ$, steady state)

Multilevel Analysis *hp-MGS* Algorithm, Stretched Meshes

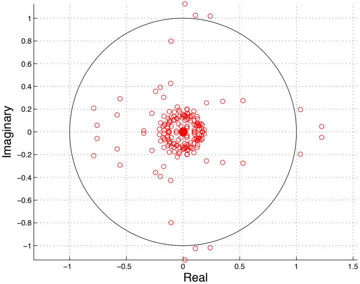

TLA-*hpMGS(1)*

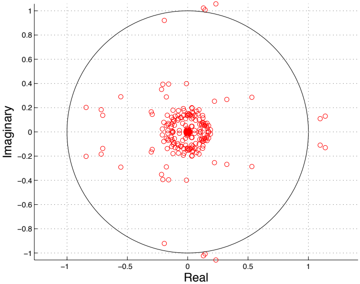

TLA-*hp*

Spectra of error transformation operator of the *hp-MGS(1)* and *hp-MGS* algorithms.

($Re_{h_1} = 10^{-1}$, $Re_{h_2} = 10^{3}$, $A_h = 100$, $\alpha = 75^\circ$, steady state)

Spectra Time-Accurate Problems

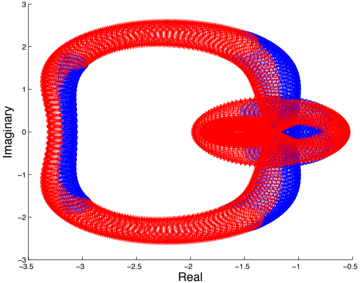

Eigenvalues $L_{h,1}$

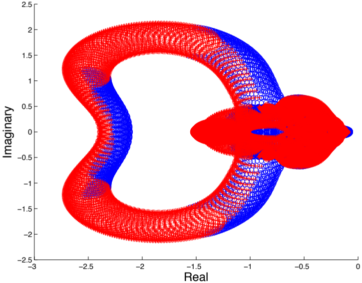

Eigenvalues $L_{h,3}$

Spectra of DG matrices $L_{h,p}$ for $p = 1$ and 3.

$CFL = 1$, $A_h = 1$, $Re_{h_1} = Re_{h_2} = 10^5$, flow angle 75°, $\rho(M_{nh,p}) = 2. \times 10^{-18}$, $\|M_{nh,p}\| = 2. \times 10^{-18}$.

UNIVERSITY OF TWENTE.

MESA+
INSTITUTE FOR NANOTECHNOLOGY

Spectra Time-Accurate Problems

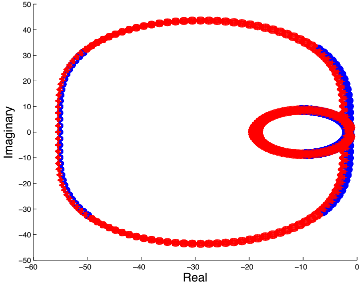

Eigenvalues $L_{h,1}$

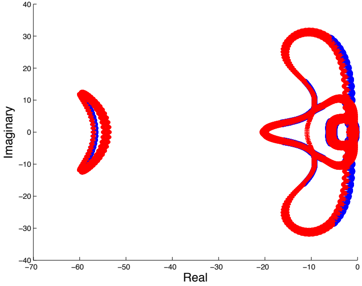

Eigenvalues $L_{h,3}$

Spectra of DG matrices $L_{h,p}$ for polynomial orders $p = 1$ and 3.

$(CFL = 1$, $A_h = 100$, $Re_{h_1} = 10^{-1}$, $Re_{h_2} = 10^3$, flow angle 75°,
$\rho(M_{nh,p}) = 2. \times 10^{-18}$, $\|M_{nh,p}\| = 2. \times 10^{-17}$.

Model Problems on Non-Uniform Mesh

- In order to test the performance for boundary layer problems we consider the advection-diffusion equation on $[0, 1]^2$ with Dirichlet and Neumann boundary conditions.

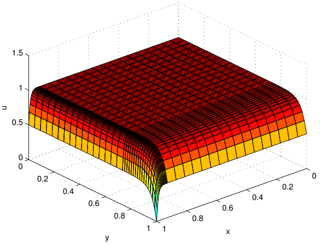

$Re = 100$, $\alpha = 15°$.

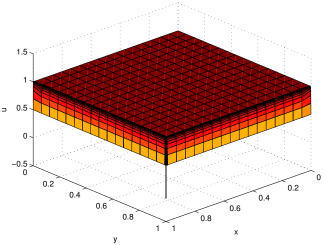

$Re = 1000$, $\alpha = 45°$.

Solution of advection-diffusion equation on a 32×32 Shishkin mesh .

- Based on the local Re_h number in each element the best RK-coefficients are selected.

Convergence Rate Original Multigrid Scheme

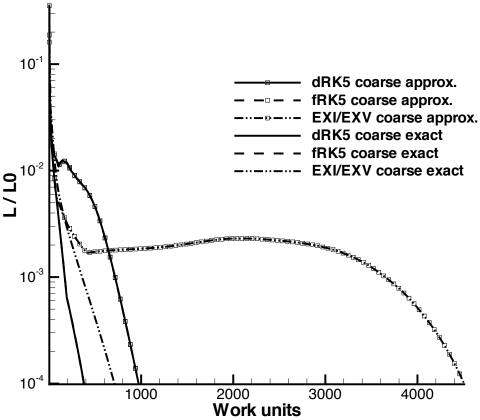

Convergence rate of original multigrid algorithm for 4th order DG discretization advection-diffusion equation ($Re = 10$, $\alpha = 22.5°$)

Mesh Dependence of Multigrid Convergence Rate

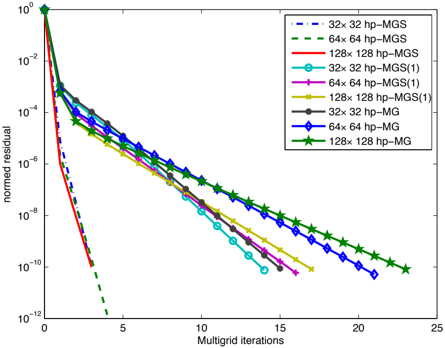

Mesh dependence of convergence rate of multigrid algorithm for 4th order DG discretization of advection-diffusion equation ($Re = 1000$, $\alpha = 45^\circ$)

Re-Dependence of Multigrid Convergence Rate

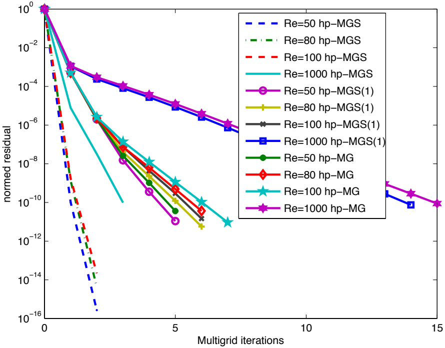

Reynolds dependence of convergence rate of multigrid algorithm for 4th order DG discretization of advection-diffusion equation (32×32 mesh, $\alpha = 45°$)

α-Dependence of Multigrid Convergence rate

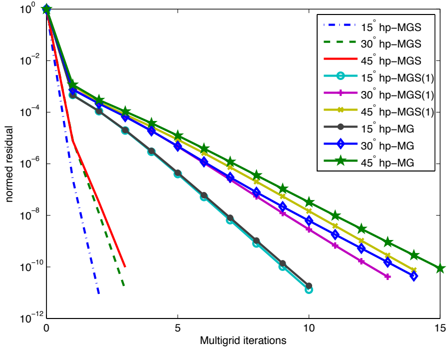

Flow angle dependence of convergence rate of multigrid algorithm for 4th order DG discretization of advection-diffusion equation (32×32 mesh, $Re = 1000$)

Rotating Flow Field

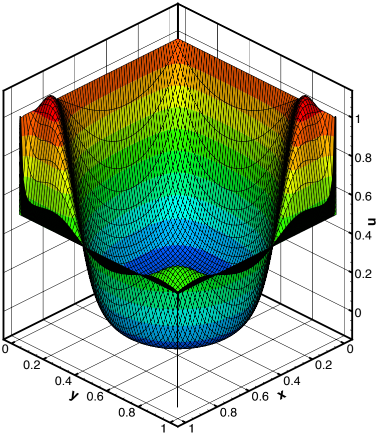

Solution of the advection-diffusion equation at $Re = 1000$ on a 128×128 Shishkin mesh for a rotating advective velocity field.

Mesh Dependence of Multigrid Convergence Rate

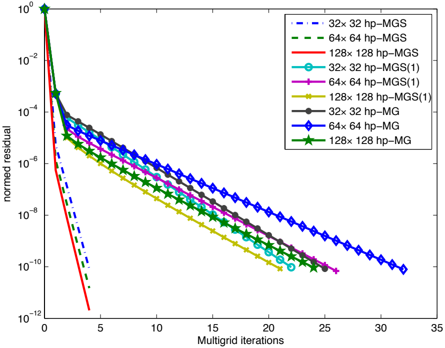

Grid dependence of convergence rate of the *hp-MGS* algorithm for a 4th order accurate space-time DG discretization of advection-diffusion equation at $Re = 1000$ for a rotating velocity field.

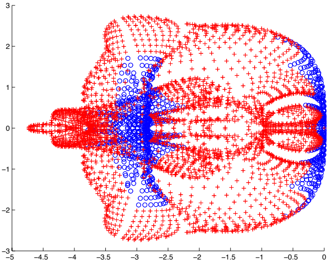

Eigenvalues $L_{h,1}$

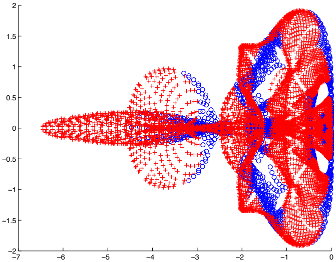

Eigenvalues $L_{h,2}$

Spectra of DG matrices $L_{h,p}$ for $p = 1$ and 2 ($Ma = 0.4$, $A_h = 1$, $\alpha = 45^\circ$).

Multilevel Analysis *hp-MGS* Algorithm – Euler Equations

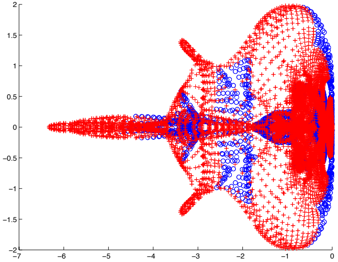

Eigenvalues $L_{h,3}$

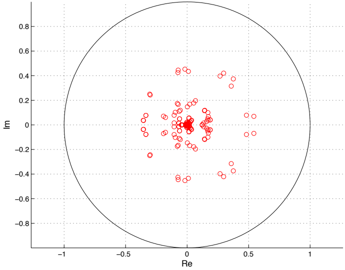

TLA-*hpMGS*

Spectrum of DG matrix $L_{h,3}$ and the error transformation operator of the *hp-MGS* algorithm ($Ma = 0.4$, $A_h = 1$, $\alpha = 45^\circ$).

Conclusions

The *hp-MGS* algorithm combines a number of innovations:

- The use of a semi-coarsening *h-MGS* algorithm as smoother at all *p*-multigrid levels.
- A new semi-implicit Runge-Kutta smoother with optimized coefficients.
- The use of discrete Fourier analysis of the complete *hp-MGS* algorithm in two-space dimensions to analyze and optimize the algorithm.

Conclusions

- The *hp-MGS* algorithm shows an excellent convergence rate for both advection and diffusion dominated solutions of the advection-diffusion equation, including thin boundary layers.

- The larger computational cost of the *hp-MGS* algorithm, compared to standard *hp*-multigrid, is more than compensated by its faster convergence rate and robustness.

Outlook

- The optimization algorithm currently is used to optimize the multigrid performance for the compressible Euler and Navier-Stokes equations.
- Extensions to unstructured meshes with mixed hexahedral and prismatic space-time elements are being tested. These *hp-MGS* algorithms heavily rely on the ability of discontinuous Galerkin discretizations to deal with nonconforming meshes.

References

- J.J.W. van der Vegt and S. Rhebergen, *HP-multigrid as smoother algorithm for higher order discontinuous Galerkin discretizations of advection dominated flows. Part I. Multilevel Analysis.* Journal of Computational Physics 231, pp. 7537-7563, 2012.

- J.J.W. van der Vegt and S. Rhebergen, *HP-multigrid as smoother algorithm for higher order discontinuous Galerkin discretizations of advection dominated flows. Part II. Optimization of the Runge-Kutta smoother.* Journal of Computational Physics 231, pp. 7564-7583, 2012.

- J.J.W. van der Vegt and S. Rhebergen, Discrete Fourier analysis of multigrid algorithms. Memorandum 1957, Department of Applied Mathematics, University of Twente, Enschede, 2011.